INTERNATIONAL JOURNAL OF MECHANICAL ENGINEERING AND TECHNOLOGY (IJMET)

ISSN 0976 – 6340 (Print)
ISSN 0976 – 6359 (Online)
Volume 4, Issue 3, May - June (2013), pp. 191-202
© IAEME: www.iaeme.com/ijmet.asp
Journal Impact Factor (2013): 5.7731 (Calculated by GISI)
www.jifactor.com

IJMET
© I A E M E

FEM BASED MODELLING OF AMB CONTROL SYSTEM

Madhura.S[†], Pradeep B Jyoti[††], Dr.T.V.Govindaraju[†††],

[†]lecturer, Mechanical Engineering Department, ShirdiSai Engineering College, Bangalore, India
[††]Head of The Electrical Engineering Department, ShirdiSai Engineering College, Bangalore, India
[†††]Principal, ShirdiSai Engineering College, Bangalore, India

ABSTRACT

Active Magnetic Bearing (AMB) sustains a rotor by magnetic attractive forces, exclusive of any mechanical contact. This paper illustrates a field-circuit design of an active magnetic bearing in conjunction with its control loop. The primary and underlying specifications of the active magnetic system have been realized from a FEM study of a magnetic bearing actuator. The position control system is grounded on working dynamics of the local accustomed PID controller, which has been extensively employed in manufactories oriented employment of the active magnetic bearing systems. The specifications of the controller have been acquired by exploiting the root locus method. The realized simulation and experimental outcomes are evaluated in event of lifting the rotor.

Keywords: Modelling, control system, magnetic bearing control system, Finite Element Method, controller, simulation, rotor, levitation control algorithm, force, flux density transfer function, transmittance.

1. INTRODUCTION

Active magnetic bearings assert employment in abstruse and industrial appliances to sustain the contactless levitation of the rotor. Resolute working of apparatuses and machines, which comprise of active magnetic bearings are realized by virtue of appurtenant magnetic forces developed by the magnetic bearing actuator. Magnetic bearings have quite a few leverages over mechanical and hydrostatic ones. The uttermost important improvements are

[9]: contactless dynamics and exemption from lubrication and contamination wear. The rotor may be conceded to rotate at high speed; the immense circumferential speed is only restrained by the tenacity and stableness of the rotor material and constituents. At high operation speeds, friction losses are diminished by 5 to 20 times than in the prevailing ball or journal bearings. Considering the dearth of mechanical wear, magnetic bearings have superior life span and curtailed maintenance expenditure. Nonetheless, active magnetic bearings also have its shortcomings. The contrivance of a magnetic bearing system for a specialized employment necessitates proficiency in mechatronics, notably in mechanical and electrical engineering and in information processing. Owing to the intricacies of the magnetic bearing system, the expenses of procurement are considerably larger vis-a-vis conventional bearings. Howbeit, on account of its many superiorities, active magnetic bearings have asserted acceptance in many industrial applications, such as turbo-molecular vacuum pumps, flywheel energy storage systems, gas turbines, compressors and machine tools.

With the aid of this thesis, the dynamic behavior of an active magnetic bearing has been scrutinized. The illustrated dynamic model is grounded on the coil inductance, the velocity-induced voltage coefficient and the radial force characteristic, which are computed by the finite element method.

2. MODELLING OF THE ACTIVE MAGNETIC BEARING

2.1 Specification

The deliberate levitation actuator produces a 12-pole heteropolar bearing. The magnetic system has been fabricated from laminated sheets of M270-50 silicon steel. Organization of the 12-pole system is disparate from the 8-pole archetypical bearings. The attractive force produced in y-axis is twice the force generated in the x-axis. The four control windings of the 12-pole bearing, exhibited in Figure 1, comprises of 12 coils connected thusly: 1A-1B-1C-1D,2A-2B, 3A-3B-3C-3D and 4A-4B. The windings 1 and 3 generates the attractiveforce along the y -axis, albeit windings 2 and 4 generate magnetic force in the x-axis. The physical characteristics of the active magnetic bearing have been exhibited in Table 1.

TABLE 1

Specification of the radial active magneticbearing parameters

Property	**Value**
Number of Poles	12
Stator axial length	56 mm
Stator outer diameter	104 mm
Stator inner diameter	29 mm
Rotor axial length	76 mm
Rotor diameter	28 mm
Nominal air gap	1 mm
Number of turns per pole	40
Copper wire gauge	1 mm2
Stator weight	2.6 kg
Current stiffness coefficient	13 N/A
Position Stiffness coefficient	42 N/mm

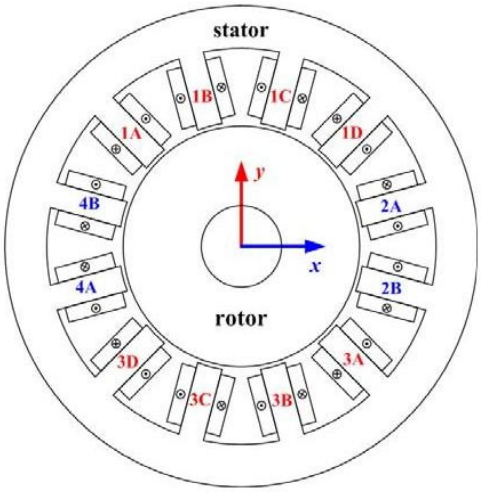

Fig. 1. Front view of the active Magnetic bearing

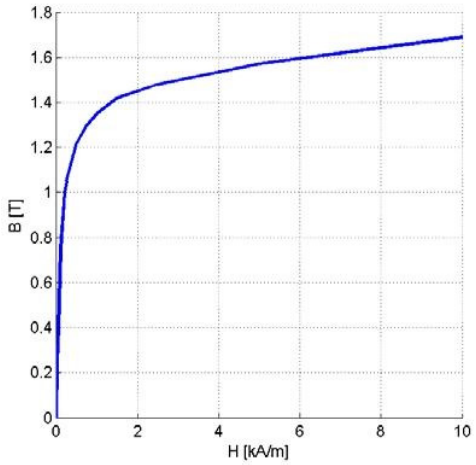

Fig. 2. B-H characteristic for the laminated ferromagnetic material M270-50

2.2. Modelling of the active magnetic bearing actuator

Active magnetic bearing is an archetypical electromagnetic system where the electrical and mechanical energies are conjugated by the magnetic field. A dynamic representation of the active magnetic bearing in y-axis is governed by the assortment of ordinary differential equations:

$$u_1 = R_1 i_1 + L_{d1} \frac{di_1}{dt} + h_{v1} \frac{dy}{dt} \quad (1)$$

$$u_3 = R_3 i_3 + L_{d3} \frac{di_1}{dt} + h \frac{dy}{dt} \quad (2)$$

$$m \frac{d^2 y}{dt^2} = F_y(i_{cy}, y)$$

The voltage equations (1) actuates the electrical comportment of the active magnetic bearing, wherein u1, u 3 are the supply voltages, the currents i1, i3 consist of bias and control ones: i1 = iby + icy, i3 = iby - icy. R1, R3 are the winding's resistances, Ld1, L d3 designate the dynamic inductances of the windings and hv1, hv3 elucidates the velocity-induced voltage. The mechanical equations (2) actuates the dynamic model of the magnetically suspended shaft.

An active magnetic bearing is identified by the nonlinear affiliation between the attractive force and position of the rotor and windings currents.

Scrutinizing the opposing pair of the electromagnets the subsequent linear correlation for the attractive force can be realized:

$$F_y = k_{iy} i_{cy} k_{sy} y \tag{3}$$

The current stiffness coefficient k_{iy} and position stiffness coefficient k_{sy} are construed as partial derivatives of the radial force $F_{y,}$ [10]:

$$k_{iv} = \frac{\partial F_v(i_{cv,} y)}{\partial i_{cv}}_{y=o}, k_{sv} = \frac{\partial F_v(i_{cv,} y)}{\partial y}_{i_{cv}=0} \tag{4}$$

The fundamental specifications of the active magnetic bearing actuator have been enumerated using FEM analysis. Simulation of the magnetic bearing was actualized with Matlab/Simulink software. The block diagram of the AMB model in the *y*-axis for the field-circuit method is illustrated in Figure 3. The constituents of the block "Electromagnets 1 and 3" is shown in Figure 4.

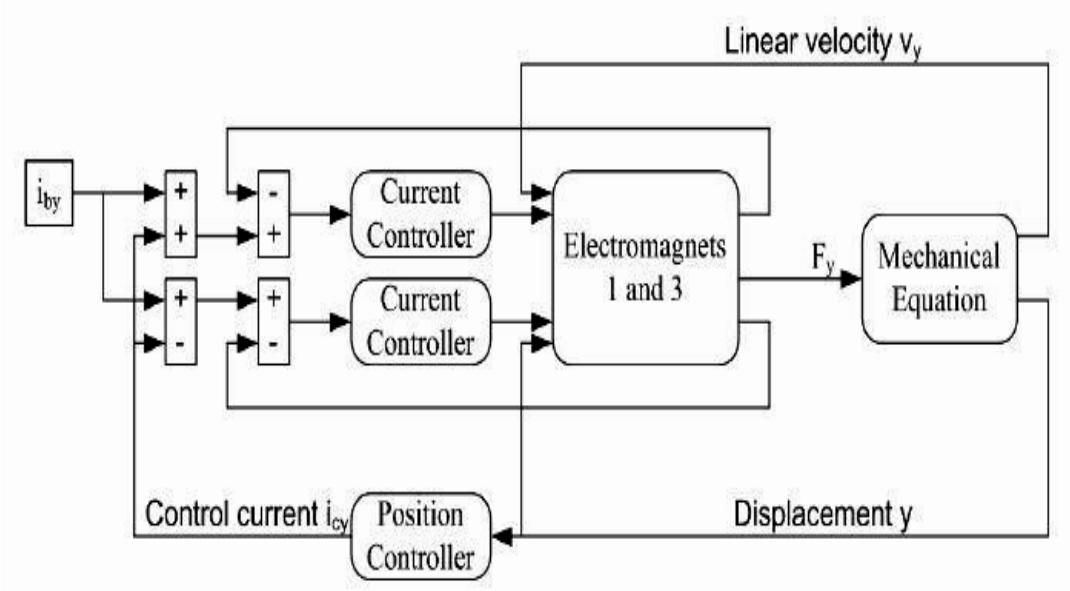

Fig. 3. Block diagram for the analysis of the AMB dynamics in *y*-axis

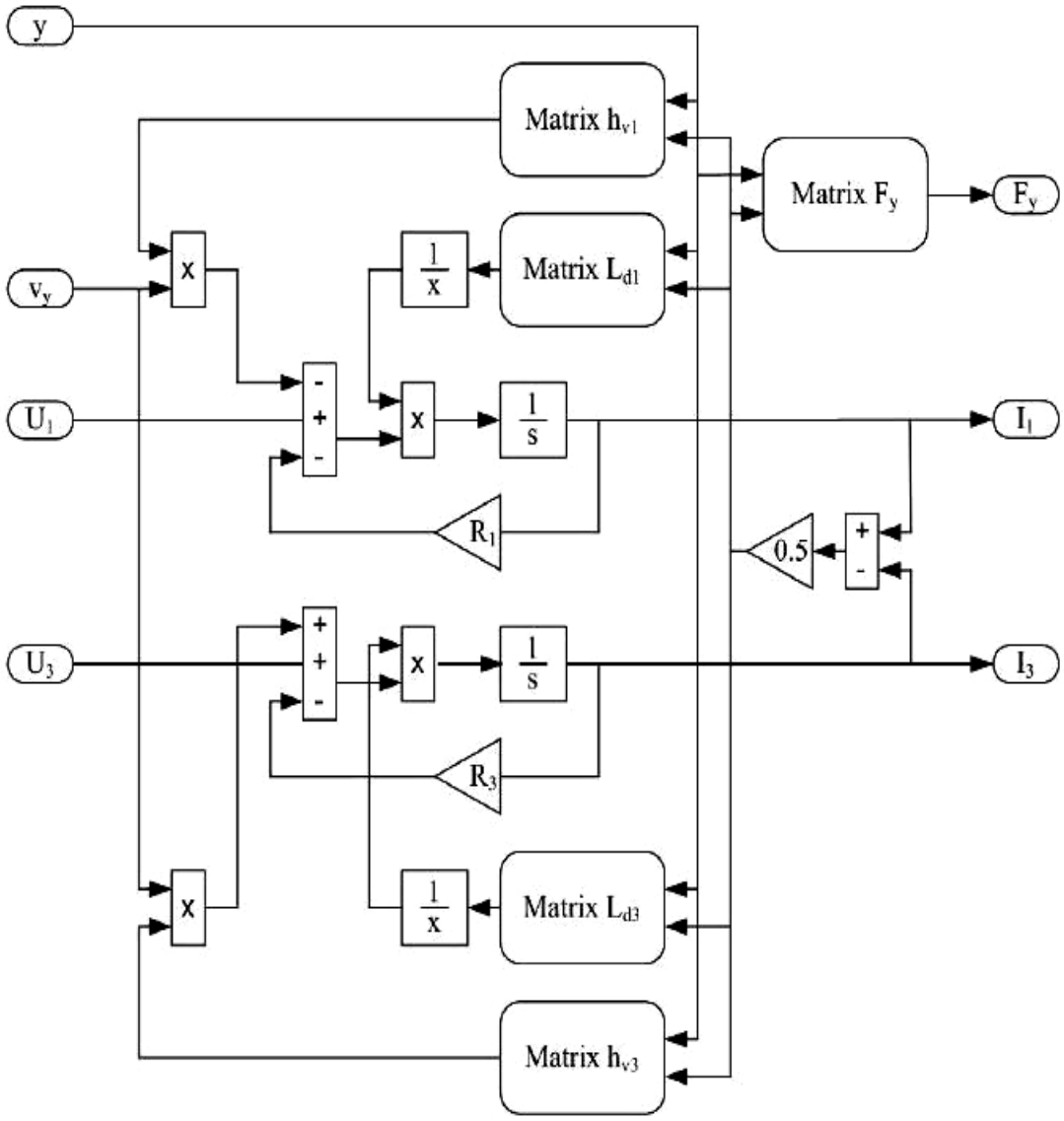

Fig. 4. The content of the block Electromagnets 1 and 3"

2.3. Finite element computation of AMB

Magneto static estimation of magnetic field distribution in the magnetic bearing was executed by 2D Finite Element Method, employing the program FEMM 4.2 [8]. The problem is formulated by Poisson's equation:

$$\nabla \times \left\{ \frac{1}{\mu \vec{B}} \nabla \times \vec{A} \right\} = \vec{J}$$

Where μ is the permeability of material, B is the magnetic flux density, A is the magnetic vector potential in z direction, J is the current density. In the calcu- lation incorporates nonlinear characteristics $\mu(B)$ of the ferromagnetic material, illustrated in Figure 2. A two-dimensional mock up of the active magnetic bearing has been discredited by 82356 standard triangular

elements(Fig. 5a). Computation of the magnetic bearing forces by the Maxwell's stress tensor method necessitates a closed surface that envelopes the rotor in free space [1]. For that reason, the air gap area was split into two subareas amidst stator and rotor (Fig. 5b). In consideration of solving equation (5) the boundary conditions have to be ascertained. As a result, on the outer edges of the calculation area Dirichlet boundary conditions have been assumed.

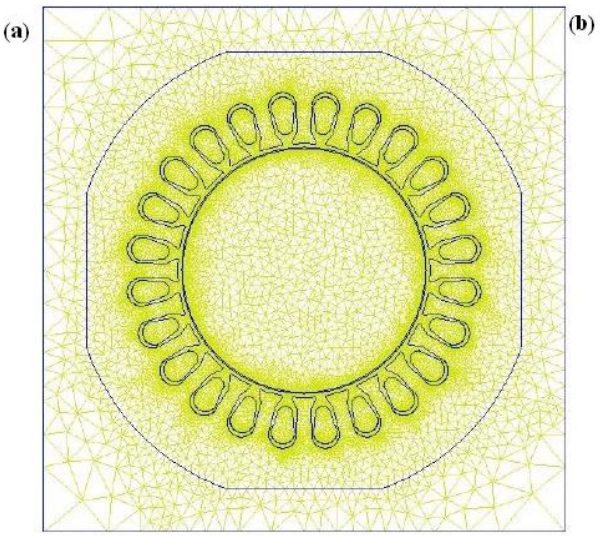

Fig. 5.Discretization of the model

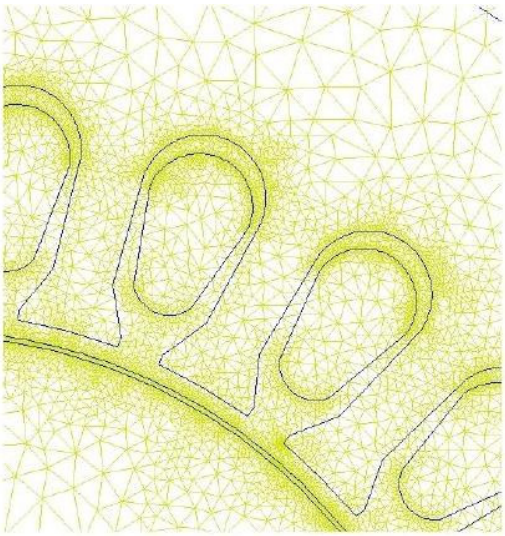

Fig. 6. The finite element mesh in the subregions of stator and rotor

In light of equation (5) solution, the circulation of the A_z component for magnetic vector potential has been realized. Consequently, the vector of magnetic field distribution is ascertained as:

$$\vec{B} = \frac{\partial A_z}{\partial y} 1_x - \frac{\partial A_z}{\partial x} 1_y \qquad (6)$$

Assuming the 2D field, the magnetic flux of the coils has been calculated from:

$$\Psi = \sum_{i=1}^{N} \oint_l \vec{A}.\vec{dl} = \sum_{i=1}^{N} l_1 (A_{zj+} - A_{zj-}) \qquad (7)$$

where*N* connotes the number of turns of the coil, $A_{z,i+}$ and $A_{z,i-}$ are the vector potentials on the positive and negative sides of the coil turn, correspondingly.

The dynamic inductance is calculated as partial derivative of the flux with respect to the current *i*:

$$L_d = \frac{\overline{\partial \psi}}{ol} \qquad (8)$$

while the velocity-induced voltage is derived as partial derivative of the flux with respect to the displacement *s*:

$$h_v = \frac{\overline{\partial \psi}}{os} \tag{9}$$

The displacement "*s*" connotes "*y*" or "*x*" movement. The radial force is derived by Maxwell's stress tensor method, in which the electromagneticforce is deduced as surface integral:

$$F = \frac{1}{2}\int \{\overline{H}(\overline{n}.\overline{B}) + \overline{B}(\overline{n}.\overline{H}) - \overline{n}(\overline{H}.B)\}ds \tag{10}$$

where H is the magnetic field intensity and n is the unit surface perpendicular to S .

The flux density plot for control currenti_{cy} = 4 A,i_{cx} = 0 A and at the central position of the rotor (x = y = 0 mm) is illustrated in Figure 7. Under these circumstances, the active magnetic bearing produces maximum radial force in the *y*-axis, while the component in *x*-axis is zero. An average value of the flux density in the pole tooth is 1.30 T.

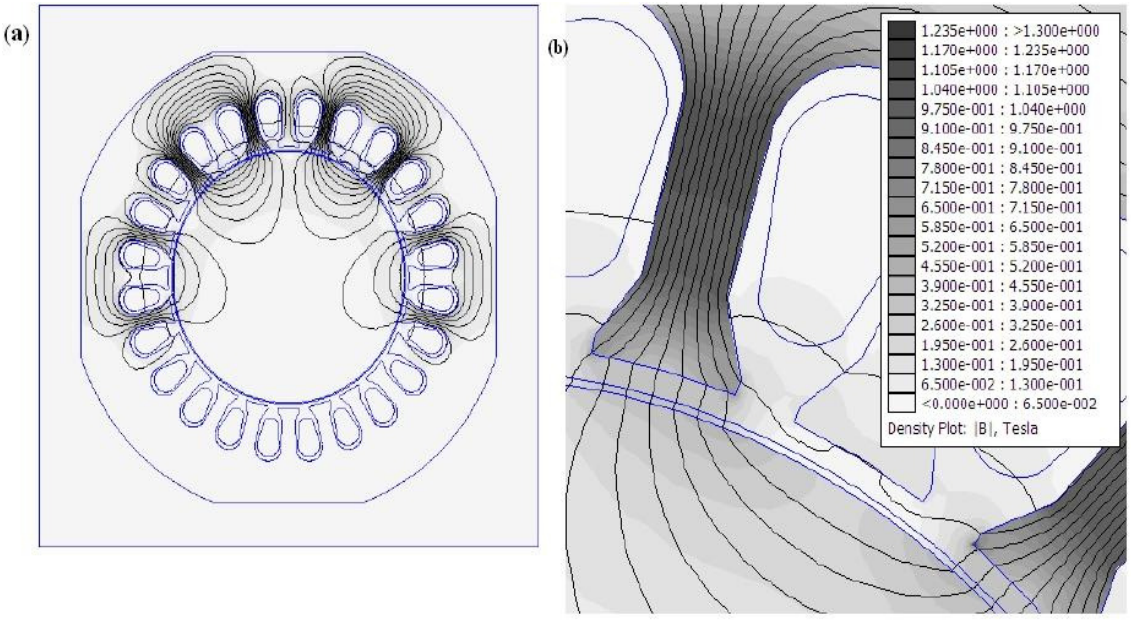

Fig. 7. Magnetic field distribution for the casei_b = 4 A,i_{cy} = 4 A,i_{cx} = 0 A and x = y = 0 mm in whole geometry of active magnetic bearing (a) and in the pole teeth (b)

Characteristics of radial force F_y and fluxesΨ_1,Ψ_3 in the coils have been actualized over the entire operating scopei_{cy}∈(-4.0 A, 4.0 A), y∈(-0.3 mm, 0.3 mm). The radial forceF_y and fluxΨ_1 characteristics are illustrated in Figure 8 and Figure 9.

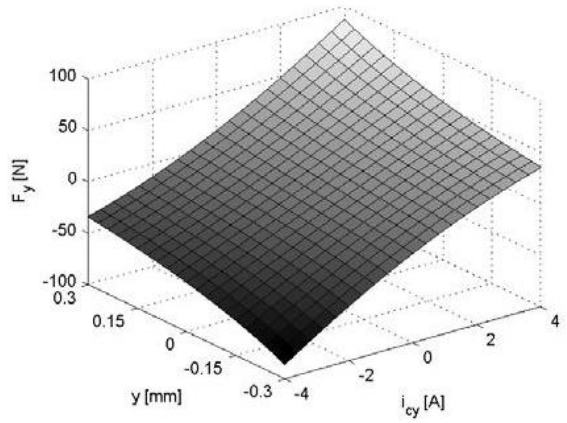

Fig. 8. Radial force characteristic $F_y(i_{cy},y)$

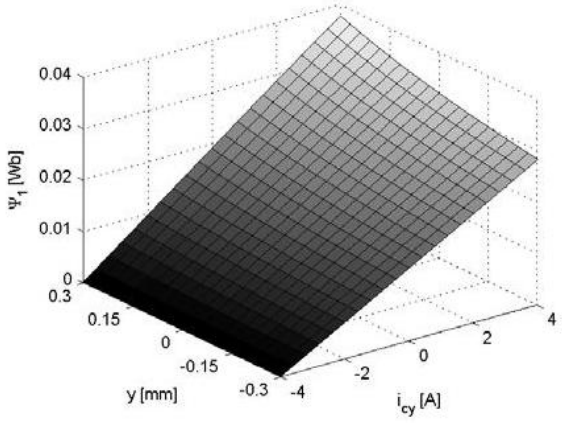

Fig. 9. Flux characteristic $\Psi_1(i_{cy},y)$

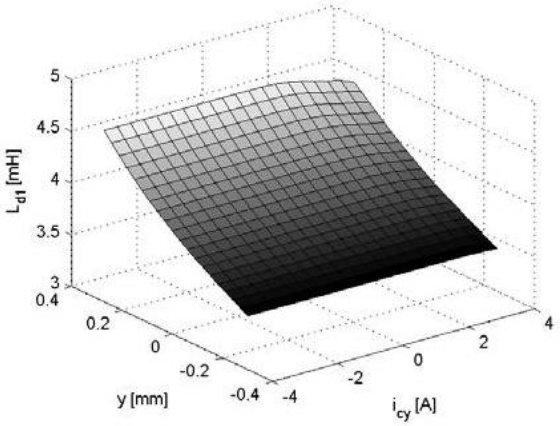

Fig. 10. Dynamic inductance characteristic $L_{d1}(i_{cy},y)$

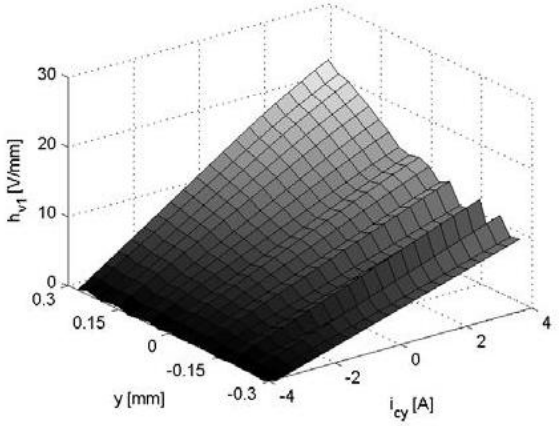

Fig. 11. The velocity-induced voltage char- acteristic $h_{v1}(i_{cy},y)$

2.4. Control system for the Active Magnetic Bearing

Lately there have been new developments and improvisation of various algorithms to manipulate the active magnetic bearings. The most decisive and momentous ones are: PID control [4], gain scheduled control [2], robust H_∞ control [6], LQ control [11], fuzzy logic control [5], feedback linearization control [7]. Regardless of comprehensive and accelerated development of the advanced control algorithms for the active magnetic bearing, the industrial applications of the magnetic bearing were generally grounded on digital or analog PID controllers.

The transformation function of the current controlled active magnetic bearing in *y*-axis is governed by the following equation:

$$G_{AMB}(s) = \frac{k_{iv}}{ms^2 - k_{sv}} \qquad (11)$$

The poles of the transfer function exemplifies an unstable system, since one of the poles has a positive value. Therefore, the active magnetic bearing necessitates a control system. Stable fuctioning can be realized with decentralized PID controller, with the transfer function [3]:

$$G_{PID}(s) = K_p + K_{I_s} + sK_D \tag{12}$$

The block diagram of the control system with PID controller for *y*-axis is illustrated in Figure 12, where $y_r(t)$ connotes the reference value of the rotor position (generally equal to zero), $i_{cy}(t)$ is the reference control current and $y(t)$ is position of the rotor.

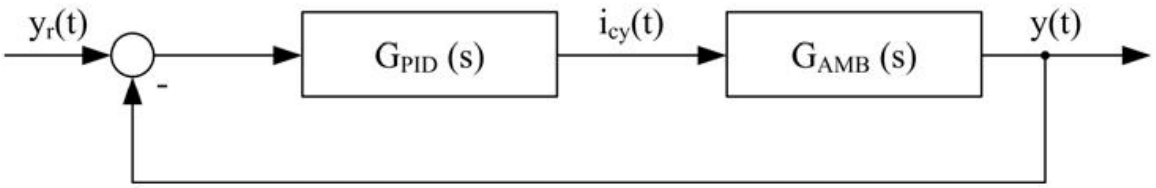

$$G_{CL}(s) = \frac{\frac{K_D k_{iy}}{m} S^2 + \frac{Kpk_{iy}}{m} S + \frac{K_I k_{iy}}{m}}{S^3 + \frac{K_D k_{iy}}{m} S^2 + \frac{Kpk_{iy}}{m} S + \frac{K_I k_{iy}}{m}} \tag{13}$$

The closed-loop system with the PID controller has three poles $\lambda_1, \lambda_2, \lambda_3$. To deduce the magnitude of K_P, K_I, K_D, the coefficients of the denominator of $G_{CL}(s)$ in Eq. 13 should be evaluated against coefficients of the polynomial form:

$$s^3 + (\lambda_1 + \lambda_2 + \lambda_3)s^2 + (\lambda_1\lambda_2 + \lambda_2\lambda_3 + \lambda_1\lambda_3)s + \lambda_1\lambda_2\lambda_3 \tag{14}$$

As a result, the specifications of the PID controller are equal to:

$$K_p = \frac{(\lambda_1\lambda_2 + \lambda_2\lambda_3 + \lambda_3\lambda_1)}{k_{iv}} \tag{15}$$

$$K_I = \frac{\lambda_1\lambda_2\lambda_3 m}{k_{iv}}$$

$$K_D = \{(-\lambda_1 - \lambda_2 - \lambda_3)m\}k_{iy}$$

Position of the poles $\lambda_1, \lambda_2, \lambda_3$ in the *s*-plane influences the characteristics of the transients. According to the pole placement method [4] two poles can be determined from:

$$\lambda_1 = -\omega_n\zeta + i\omega_n\sqrt{1-\zeta_2}$$
$$\lambda_2 = -\omega_n\zeta + i\omega_n\sqrt{1-\zeta_2} \tag{16}$$

Where in ω_n is the undamped natural frequency:

$$\omega_n = \frac{4.6}{t_s \zeta} \tag{17}$$

The third pole of transfer function of $G_{CL}(s)$ should be positioned outside the dominant area. Subsiquently, the coefficients K_P, K_I, K_D rely on the settling time t_S and damping ratio ζ.

3. SIMULATION AND EXPERIMENTAL RESULTS

To stabilize the rotor two decoupled PID controllers were employed. The control tasks have been accomplished with 32-bit microcontroller with very proficient ARM7TDMI-S core. The sampling frequency of PID controllers are equal to 1 kHz. The location of the rotor is measured by Turck contact-less inductive sensor with bandwidth 200 Hz. The analog to digital converters resolution equals 2.44 μm. The parameters of PID controllers were determined accor- ding to the proposed method for the settling time t_S = 50 ms and the damping coefficient $\zeta = 0.5$. The values of parameters of PID controllers are shown in Table 2.

TABLE 2
Parameters of the PID controller

KP[A/m]	KI[A/ms]	KD[ms/m]
11231	514080	45

Figures 13 and 14 illustrate the contrast of simulated and experimental outcomes throughout rotor lifting. The curve characters of the properties are close to the measured ones. It is evident that the current value in the steady state is marginally higher than in the real system.

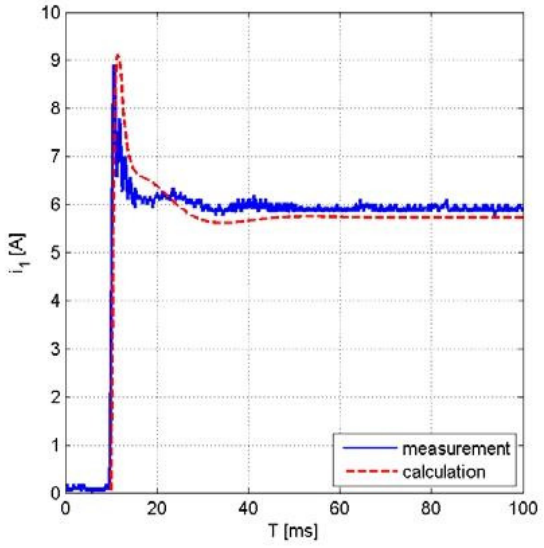

Fig. 13.Time response of current i_1

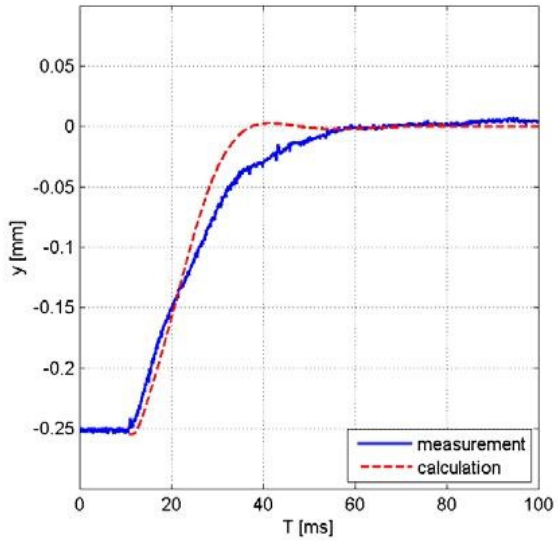

Fig. 14. Time response of the AMB shaft displacement in *y*-axis

The transient state for the rotor position for both systems diversifies, owing to the fact that the settling time in the simulated system is shorter than in the real one. Contrarieties are result of the simplified modelling of the magnetic bearing's actuator, specifically because of overlooking the hysteresis phenomena and the fringing effect.

4. REMARKS AND CONCLUSION

This thesis demonstrates a modus-operandi for designing control systems for active magnetic bearings. The dynamic behavior of active magnetic bearings has been realized from a field-circuit model. The fundamental parameters of the active magnetic bearing actuator have been deduced using FEM analysis .

The illustrated technique for designing PID controllers makes manipulating the controller specifications simpler and promises acceptable damping.

LITERATURE

[1.] Antila M., Lantto E., Arkkio A.: Determination of Forces and Linearized Parameters of Radial Active Magnetic Bearings by Finite Element Technique, IEEE Transaction On Magnetics, Vol. 34, No. 3, 1998, pp. 684-694.

[2.] Betschon F., Knospe C.R.: Reducing magnetic bearing currents via gain scheduled adaptive control, IEEE/ASME Transactions on Mechatronics, Vol. 6, No. 4, 12.2001, pp. 437-443.

[3.] FranklinG.: Feedback control of dynamic systems, Prentice Hall, New Jersey, 2002.

[4.] Gosiewski Z., Falkowski K.: Wielofunkcyjnełożyskamagnetyczne, BibliotekaNaukowa InstytutuLotnictwa, Warszawa, 2003.

[5.] Hung. J.Y.: Magnetic bearing control using fuzzy logic, IEEE Transactions on Industry Applications, Vol. 31, No. 6, 11.1995, pp. 1492-1497.

[6.] Lantto E.: Robust Control of Magnetic Bearings in Subcritical Machines, PhD thesis, Espoo, 1999.

[7.] Lindlau J., Knospe C.: Feedback Linearization of an Active Magnetic Bearing With Voltage Control, IEEE Transactions on Control Systems Technology, Vol. 10, No.1, 01.2002, pp. 21-31.

[8.] Meeker D.: Finite Element Method Magnetics Version 4.2, User's Manual, University of Virginia, U.S.A, 2009.

[9.] Schweitzer G., Maslen E.: Magnetic Bearings, Theory, Design and Application to Rotating Machinery, Springer, Berlin, 2009.

[10.] Tomczuk B., Zimon J.: Filed Determination and Calculation of Stiffness Parameters in an Active Magnetic Bearing (AMB), Solid State Phenomena, Vol. 147-149, 2009, pp. 125-130.

[11.] Zhuravlyov Y.N.: On LQ-control of magnetic bearing, IEEE Transactions On Control Systems Technology, Vol. 8, No. 2, 03.2000, pp. 344-355.

[12.] H. Mellah and K. E. Hemsas, “Design and Simulation Analysis of Outer Stator Inner Rotor Dfig by 2d and 3d Finite Element Methods”, International Journal of Electrical Engineering & Technology (IJEET), Volume 3, Issue 2, 2012, pp. 457 - 470, ISSN Print : 0976-6545, ISSN Online: 0976-6553.

[13.] Siwani Adhikari, “Theoretical and Experimental Study of Rotor Bearing Systems for Fault Diagnosis”, International Journal of Mechanical Engineering & Technology (IJMET), Volume 4, Issue 2, 2013, pp. 383 - 391, ISSN Print: 0976 – 6340, ISSN Online: 0976 – 6359.

AUTHORS DETAIL

Madhura.S

Obtained her BE from Visveswaraya Technological University in the year 2008, ME in Machine Design from Anna University. Coimbatore in the year 2011.Currently Pursuing Ph.D – Failure analysis of Active Magnetic Bearing and its correction using smart controller under the guidance of Dr.T.V.Govindaraju.Field of interest Machine design, FEM techniques and mechatronics.

Pradeep B Jyoti

Graduated from Karnataka University Dharwad, Karnataka in the year 1986, M.E from Gulbarga University, Gulbarga in the year 1989. He is currently pursuing Ph.D at Jawaharlal Nehru Technological University, Hyderabad, India. He is presently working as Professor & Head in the Department of Electrical and Electronics ShirdiSai Engineering College, Bangalore, Karnataka, India. His research areas include SVPWM techniques, and Vector control of electrical drives & machines.

Dr.T.V.Govindaraju

Obtained his Ph.D in the field of" experimental techniques (photo elasticity)" in the year 2000 from Bangalore University. His current field of interest are Machine design, FEM techniques and Mechatronics. Presently involved in guiding Research scholars leading to Ph.D program.